https://doi.org/10.5194/egusphere-2025-5855
Preprint. Discussion started: 8 January 2026

Evaluating Different Roughness Approaches and Infiltration Parameters for Vegetation-Influenced Overland Flow in Hydrological Model

Azam Masoodi[1], Philipp Kraft[1]
[1]Department of Landscape Ecology and Resources Management, Justus Liebig University Giessen, 35392, Germany
Correspondence to: Philipp Kraft (philipp.kraft@umwelt.uni-giessen.de)

Abstract. Accurately simulating overland flow in vegetated landscapes remains a challenge in hydrological modeling due to the complex interactions between vegetation, surface roughness, and soil infiltration. This study evaluates multiple methods for estimating Manning's roughness coefficient and explores the influence of vegetation on infiltration processes using the OpenLISEM model. Based on 132 artificial rainfall experiments across 22 sites in southwest Germany, the model was calibrated and validated against observed runoff data, incorporating both depth-independent and depth-dependent roughness formulations. Incorporating water depth-dependent roughness into the model can improve its performance in simulating overland flow. Beyond roughness effects, vegetation was shown to significantly alter soil hydraulic properties, particularly saturated hydraulic conductivity (Ksat). Paired site comparisons revealed that increased vegetation cover corresponded with higher infiltration capacities, emphasizing vegetation's role not only in surface resistance but also in enhancing subsurface water fluxes. The findings demonstrate that models must account for both surface and subsurface impacts of vegetation to improve runoff predictions.

1 Introduction

Overland flow is a critical component of the hydrological cycle, playing a significant role in flood generation, soil erosion, and pollutant transport. Accurate overland flow modelling is essential for effective water resource management, flood prediction, and environmental protection. Accurately representing the effects of vegetated areas remains one of the primary challenges in overland flow modelling, as these areas play a critical role in the hydrological cycle (Peel, 2009). Vegetation significantly influences flow dynamics by increasing surface roughness, modifying flow patterns, and providing additional drag (Zhang et al., 2018). Beyond these hydrodynamic effects, vegetation also changes the infiltration regime, thereby the partitioning between infiltration and overland flow (Ajayi et al., 2021).

The hydrodynamic effects of vegetation on flow vary significantly between emergent and submergent plant communities, with distinct hydrodynamic impacts based on their structural characteristics and interaction with water depth (D'Ippolito et al., 2021). As vegetation density increases, it slows flow velocity and can reduce the erosive power of surface runoff (Mu et al., 2019). The interaction between vegetation and overland flow is often quantified through roughness coefficients, with Manning's coefficient being one of the most widely used parameters in hydrological modelling. At present, roughness parameters for overland flow are derived mainly from field measurements and laboratory experiments (Oberle et al., 2024).

Recent studies have shown that roughness coefficients are not constant but vary with factors such as water depth, vegetation density, and flow velocity (Ruiz Rodriguez, 2017; Fu et al., 2019; Hinsberger et al., 2022). Hinsberger et al. (2022) performed laboratory experiments to investigate roughness variations in submerged and emergent vegetation, demonstrating that increased submergence reduces roughness, whereas for emergent vegetation, greater submergence leads to heightened roughness. Their findings suggested that roughness-water depth relationships for intermediate zones can be approximated using a linear approach. Feldmann et al. (2023) proposed a framework to estimate Manning roughness dependent on shallow water depth. First, the partitioning of overland flow and infiltration was calculated during the descending limb of the hydrograph to determine the minimum infiltration rate. Then, they reduced the solution space by comparing experiments

https://doi.org/10.5194/egusphere-2025-5855
Preprint. Discussion started: 8 January 2026

conducted at one site and by comparing sites with similar properties. The framework's robustness was tested using three different depth-dependent roughness equations and a constant Manning coefficient.

Utilizing flow resistance models in vegetated areas holds immense value in evaluating the potential for flooding and formulating flood mitigation strategies grounded in scientific principles (Green, 2005). However, evaluating these equations to calculate overland flows continues to be a staple area of research within hydrology. The uncertainty associated with roughness coefficients can significantly impact surface runoff accumulation. For example, Dalledonne et al. (2019) introduced an approach to evaluate uncertainty in floodplain hydrodynamic models influenced by vegetation, testing four resistance formulas. Oberle et al. (2021), carried out a review on flow resistance in overland flow. Based on some previous laboratory experiments concerning artificial grass, they demonstrated that the roughness function varies with water depth in the presence of vegetation. They noted that uncertainties emerge as the cross-sectional impact of vegetation elements is usually not considered in the calculation of resistance coefficients. In contrast, Luhar and Nepf (2013) investigated the effect of vegetation distribution on channel velocity, presenting physically based models that link drag generated by vegetation at the blade and patch scale to hydraulic resistance. This resistance depends on the blockage factor, which represents the fraction of the channel cross-section occupied by vegetation. However, the applicability of their approach to overland flow is examined in this study. These findings highlight the need for further evaluation of roughness estimation methods under varying hydrological conditions.

On the other hand, vegetation and root systems influences soil structure, creates preferential flow paths, which promote infiltration and reduce overland flow (Ajayi et al., 2021; Jarvis et al., 2013). Gao et al. (2023) stated that the most established hydrological theories, such as those presented by Drewniak (2019) and Lu et al. (2019), predominantly parameterize water fluxes based on soil properties, including texture, porosity, moisture retention capacity, wilting point, and plant-available water. These approaches are grounded in the assumption that soil properties govern key hydrological processes such as infiltration, drainage, and evapotranspiration. In traditional modelling approaches, infiltration parameters are often estimated using soil texture-based pedotransfer functions as a primary input when direct measurements are unavailable. Gao et al. (2023) challenge this perspective, suggesting instead that this causality is misrepresented: soil properties should be viewed as outcomes rather than drivers of water movement, which is fundamentally regulated by the dynamics of the surrounding terrestrial ecosystem. Neglecting key site factors, such as land use, in parameter estimation routines can introduce significant errors in the partitioning of infiltration and runoff in hydrological modelling (Jarvis et al., 2013). The impact of vegetation cover on infiltration properties such as saturated hydraulic conductivity remains insufficiently implemented in surface runoff models. Understanding the vegetation effects on soil parameters is crucial for improving the accuracy of hydrological models. In surface runoff models, saturated hydraulic conductivity is often calibrated to align with observed data, indirectly capturing the influence of vegetation on soil properties. This study explores whether such calibrated values can implicitly reflect the influence of vegetation on soil hydraulic properties. The scope of our research encompasses the following objectives:

- Modelling the overland flow to compare and validate different approaches for Manning's coefficient estimation.
- Evaluation of overland flow model performance in estimating infiltration in the presence of vegetation

By addressing these objectives, our research contributes to improving the accuracy of hydrological models and enhancing our understanding of overland flow dynamics in vegetated areas. By utilizing the experimental dataset and hydrodynamic simulation, this study assesses the accuracy of roughness coefficient estimations in a hydrological model in a realistic environment. This assessment covers a variety of scenarios involving different levels of vegetation coverage and vegetation height and varying rainfall intensities. By providing insights into the most effective approaches for estimating surface roughness and understanding the interactions of vegetation and infiltration, this research aims to enhance the reliability of

https://doi.org/10.5194/egusphere-2025-5855
Preprint. Discussion started: 8 January 2026

overland flow predictions and support more informed decision-making in hydrological engineering and environmental planning.

2 Materials and methods

2.1 Study site and experimental setup

To develop and evaluate overland flow models in the absence of real measurement, artificial sprinkling studies present an opportunity to investigate vegetation effects on overland flow. Ries et al. (2020) conducted 132 sprinkling experiments on natural hillslopes at 23 sites with different soil types and land use in Baden-Württemberg (Germany), one of the most extensive datasets accessible in southwest Germany. Table 1 provides information about land use, vegetation properties, and soil characteristics for each site. The experimental area was a 10 by 10-meter square, with slopes ranging from 9% to 32%. These experiments aimed to simulate a 100-year or locally observed maximum rainfall intensity event with different durations. Rainfall experiments started with Run 1 on the first day. Subsequently, Run2 – Run5 were conducted on the following day and Run 6 was carried out on the third day (Table 2).

Table 1: Properties of experimental sites and the values of constant Manning's roughness coefficient.

Site*	Slope* %	Vegetation*	Veg_height* (m)	Plant coverage* %	soil type	n (Chow)	n (Feldmann)
1	12	Pasture	0.15	100	Clay	0.05	0.58
2	18	Pasture	0.1	100	Silty loam	0.05	0.60
3	**16**	**Pasture**	**0.1**	**90**	**Loam**	**0.05**	**0.70**
4	**16**	**Mustard**	**0.15**	**40**	**Clay loam**	**0.04**	**0.45**
5	**14**	**Triticale (seeded)**	**0**	**0**	**Silty loam**	**0.03**	**0.18**
6	**21**	**Pasture**	**0.05**	**100**	**Silty loam**	**0.04**	**0.65**
7	14	Winter Barley	0.3	80	Silty loam	0.05	0.38
8	**16**	**Corn (seeded)**	**0.05**	**15**	**Sandy loam**	**0.035**	**0.13**
9	**21**	**Pasture**	**0.1**	**100**	**Sandy loam**	**0.05**	**0.58**
10	32	Pasture	0.15	100	Sandy clay loam	-	-
11	18	Pasture	0.1	80	Silty clay	0.045	0.68
12	**19**	**Pasture**	**0.15**	**100**	**Silty clay**	**0.05**	**0.65**
13	**11**	**Alfalfa**	**0.2**	**40**	**Silty clay**	**0.04**	**0.28**
14	27	Pasture	0.15	100	Silty clay	0.05	0.70
15	**14**	**Winter Barley**	**0.05**	**0**	**Clay loam**	**0.03**	**0.50**
16	**12**	**Pasture**	**0.1**	**100**	**Clay loam**	**0.05**	**0.40**
17	**14**	**Pasture**	**0.05**	**100**	**Silty loam**	**0.05**	**0.48**
18	**12**	**Alfalfa and Clover**	**0.2**	**60**	**Clay**	**0.045**	**0.38**
19	21	Pasture	0.15	100	Sandy clay loam	0.05	0.98
20	9	Corn (harvested)	0	0	Clay loam	0.03	0.05
21	14	Green Manure	0.15	50	Silty clay loam	0.04	0.35
22	12	Pasture	0.2	100	Silty clay	0.05	0.38
23	14	Corn (harvested)	0	0	Clay	0.03	0.08

* Data from Ries et al. (2020)

Pair sites

The experiments conducted at Site 10 did not produce any runoff and were not used in this study. Discharge at the outlet, rainfall intensity, and initial soil moisture were measured at a temporal resolution of 1 minute. Out of the 23 sites surveyed, 12

https://doi.org/10.5194/egusphere-2025-5855
Preprint. Discussion started: 8 January 2026

locations are paired sites, highlighted in bold in Table 1. This arrangement facilitates a direct comparison between the effects of two different land uses on runoff and infiltration. The deliberate choice of these paired sites is underscored by their proximity, with distances maintained within the threshold of less than 100 meters. For more comprehensive details of these experiments, refer to Ries et al. (2020).

Table 2: Characteristics of rainfall for experimental sites (Ries et al. 2020).

Run no.	Duration (min)	Return period (yr)	Intensity (mm hr^{-1})	Cumulative Runoff: min, max, mean (mm)
Run 1	60	100	42-76	0.0, 44.3, 13.0
Run 2	60	100	42-76	0.0, 58.6, 26.9
Run 3	30	100	82-130	0.0, 50.9, 31.7
Run 4	15	100	110-172	1.4, 30.4, 22.2
Run 5	180	worst case	44-53	0.1, 145.1, 100.6
Run 6	60	worst case	99-126	32.0, 100.1, 71.0

2.1 Model

To explore the impact of roughness on overland flow simulations, it is crucial to integrate the relationship between roughness and water depth into the model. For this purpose, OpenLISEM (Open LImburg Soil Erosion Model), which was developed based on the original LISEM (Jetten, 2002), was chosen for its modular structure, physics-based approach and accessibility of the source code, published under a free licence (GNU Public Licence v3, https://github.com/vjetten/openlisem/). It is an event-based and spatial hydrological model suitable for different sizes of catchments. It focuses on simulating runoff, sediment dynamics, and infiltration during heavy rainstorms, allowing for detailed assessments of land use changes and conservation measures (Baartman et al., 2012). The elevation model is generated with a cell size of 0.5× 0.5 meter, providing information about the gradient of each specific location in the database (Table 1). Since the surface of the experimental plots is homogeneous, the generated DEM does not include micro-depressions. So, all surface parameters that may influence overland flow are represented within Manning's coefficient. This simplification does not affect our evaluation of different roughness approaches, as the conditions are consistent across all roughness methods. The last row of the DEM, colorized black in Figure 1-a, represents the trench designed to collect runoff, positioned 40 cm below the surface as in constructed experiments. Figure 1-b illustrates the field setup from Ries et al. (2020), which measured flow at three points within the trench. In our model, discharge data is recorded at the outlet, located at the corner end of the trench. Since the trench length to the outlet in the experiments is one-third of that in our model, we compensated by tripling the water velocity in the trench through a reduction in Manning's coefficient for the trench surface.

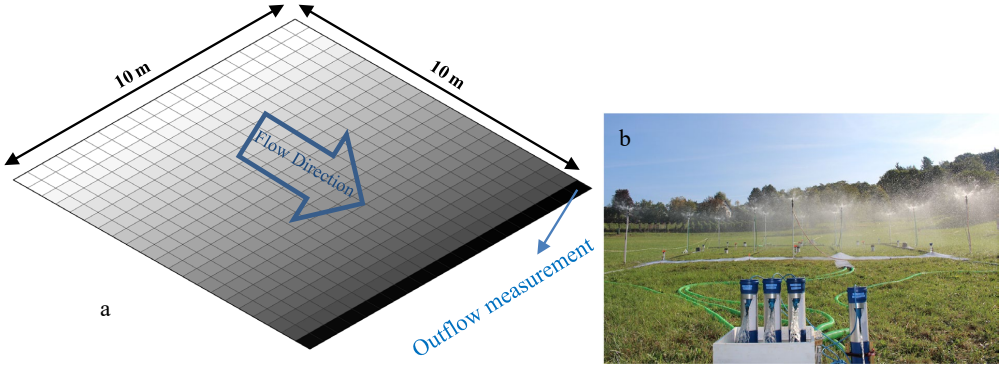

Figure 1: a) 0.5 × 0.5-meter digital elevation model applied for simulations, incorporating the specific slope of each site. b) Setup of field experiments by Ries et al. (2020).

https://doi.org/10.5194/egusphere-2025-5855
Preprint. Discussion started: 8 January 2026

Time resolution for simulation is 1second and the total simulation time is chosen based on observation runoff data.

For the distributed routing of overland flow, a four-point finite-difference solution of the kinematic wave is together with Manning's equation (Jetten, 2002). Infiltration was estimated using the Green-Ampt method (Rawls et al., 1983), which incorporates field-measured variables such as porosity and initial soil moisture content. Two additional parameters, saturated hydraulic conductivity (Ksat) and average soil suction at the wetting front (Psi), are not typically measured in the field. Prior studies, including those by Jetten (2002), Hessel et al. (2003) and Starkloff and Stolte (2014), have highlighted the primary sensitivity of OpenLISEM to Ksat and Psi parameters. Therefore, reasonable ranges for Ksat and Psi were adopted from Rawls et al. (1983), and the values were subsequently calibrated to best match observed runoff data. It should be considered that, infiltration in model depends on both soil properties and surface water depth, increased vegetation cover or a higher Manning's roughness coefficient reduces flow velocity, leading to greater surface water depth and, consequently, an enhanced infiltration rate.

OpenLISEM version 6.873 has been utilized which employs Manning's approach to calculate the runoff velocity. While the original software employed a constant Manning's coefficient as a raster map for roughness, a new feature called the dynamic Manning's n function has been introduced into the software to implement different Manning's coefficient estimation methods in simulations. This feature enables users to select from various methods of roughness estimation, including not only a constant value but also methods dependent on the depth of runoff. Detailed information about these extensions can be found in the 'Code availability.' section.

2.2 Surface roughness functions

Surface roughness functions are foundational components in the simulating of overland flow, affecting the accuracy of hydrological models. Roughness estimation approaches represent the resistance of the surface in the model that affects the momentum and energy dissipation of overland flow. In this study, two depth-independent Manning's roughness coefficients and five depth-dependent roughness functions were introduced into OpenLISEM to assess the impact of different Manning's roughness functions on vegetation modeling.

2.2.1 Constant Manning's coefficient

The initial approach assumes a constant value for Manning's roughness coefficient (n) based on Chow (1959), representing the range of flow resistance for floodplains covered by vegetations. The values of Manning's roughness coefficient using Chow's method for each site of the artificial rainfall experiments are given in Table 1. In this method, values are typically selected based on established literature or site-specific calibration. This is suitable for homogeneous surfaces and it does not consider the effect of water depth in presence of vegetation.

2.2.2 Robust Manning's coefficient

In the study conducted by Feldmann et al. (2023), the n values were directly iterated within the framework they established. The authors reported that the most robust results, characterized by high Nash-Sutcliffe Efficiency (NSE) values, were achieved with constant Manning values, as presented in Table 1. They estimate surface roughness by analyzing the shape of the hydrograph, fitting the Hortonian equation to the difference between rainfall input and observed discharge for the falling limb of the hydrograph. To achieve this goal, they assumed that the infiltration rate in the descending limb of the hydrograph is constant. For more details, see Feldmann et al. (2023).

2.2.3 Linear method

Drawing on previous literature on artificial grass, including Ruiz Rodriguez (2017), Oberle et al. (2021) concluded that a flow-depth-dependent roughness spectrum can be derived for overland flow, despite inherent variability in the data. Similarly,

https://doi.org/10.5194/egusphere-2025-5855
Preprint. Discussion started: 8 January 2026

Hinsberger et al. (2022) found Strickler coefficient, k_{Str}, values varied with different water depths in the presence of vegetation. Based on their results, there are three zones to specify roughness within the data range, categorized according to the submergence ratio: for emergent and fully submergent zones they emphasis the roughness is constant.

A linear function of relative submergence can be described for the roughness coefficient between emergent and fully submergence zones ($1 < \frac{h}{h_{veg}} < 5$ to 7) (Hinsberger et al. 2022).

These relationships are summarized in equation 1:

$$1/n_{Manning} = \begin{cases} \frac{k_{Str}}{5} & for\ 0 < h < h_{veg} \\ \frac{k_{Str}}{5} + k_{Str}\frac{h - h_{veg}}{5} & for\ h_{veg} < h < 5.h_{veg} \\ k_{Str} & for\ h > h_{veg} \end{cases} \quad (1)$$

In this study, the parameter k_{Str} is Strickler's coefficient which is estimated based on the inverse of the roughness coefficient above the vegetation using Chow (1959). Then Manning's coefficient is calculated from Eq.1, depending on the submergence ratio.

2.2.4 Luhar and Nepf's method

Another method to investigate vegetation effect on roughness was proposed by Luhar and Nepf (2013) for open channel. They suggested the following relationships between the Manning roughness caused by vegetation and blockage factor, B_x, for both submerged and emergent vegetation.

$$n_{Manning-veg} = \begin{cases} \frac{Kh^{\frac{1}{6}}}{g^{\frac{1}{2}}}\left(\frac{C_f}{2}\right)^{\frac{1}{2}}(1 - B_x)^{-\frac{3}{2}} & for\ h \le h_{veg} \text{ and } B_x < 0.8 \\ \frac{Kh^{\frac{1}{6}}}{g^{\frac{1}{2}}}\left(\frac{C_d a h}{2}\right)^{\frac{1}{2}} & for\ h \le h_{veg} \text{ and } B_x \ge 0.8 \\ \frac{Kh^{\frac{1}{6}}}{g^{\frac{1}{2}}}\frac{1}{\left(\frac{2}{C_f}\right)^{\frac{1}{2}}\left(1 - \frac{h_{veg}}{h}\right)^{\frac{3}{2}} + \left(\frac{2}{C_d a h_{veg}}\right)^{\frac{1}{2}}\left(\frac{h_{veg}}{h}\right)} & for\ h > h_{veg} \end{cases} \quad (2)$$

where $n_{Manning-veg}$ is the vegetation component of Manning's n, a is the frontal area per unit volume parameter, and C_d is drag coefficient. We assumed that the stem of vegetation is cylindrical in shape, and therefore a C_d value of 1 was used. C_f (= 0.015 - 0.19) is a coefficient to parameterize the shear stress at the interface between vegetated and unvegetated regions and the constant $K = 1\ \frac{m^{\frac{1}{3}}}{s}$ is required to make the equation dimensionally correct. The other parameters will still be the same. Although the equation was originally proposed for channel flow, this study examines its applicability to overland flow.

2.2.5 Exponential method

The exponential equation describes the relationship between n and h in terms of the variables c and d (Eq. 3).

$$n = \frac{1}{c + e^{dh}} \quad (3)$$

The optimum values of the c and d parameters for each location were derived from the study by Feldmann et al. (2023), whose proposed approach is explained in section 2.2.2.

2.2.6 Kadlec's method

Based on experimental studies on overland flow, Kadlec's power law was simplified by Jain et al. (2004) (Eq. 4).

https://doi.org/10.5194/egusphere-2025-5855
Preprint. Discussion started: 8 January 2026

$$n = n_0 \left(\frac{h}{h_0}\right)^{-\varepsilon} \quad (4)$$

where h_0 establishes the minimum flow depth, beyond which the roughness coefficient n_0 is assumed to remain constant. ε represents the influence of vegetation drag. Our study utilized the optimal values for the parameters n_0 and ε as outlined in Feldmann et al. (2023). As they did not provide information on the h_0 value, we assumed h_0 to be five times the plant height to apply the Kadlec's method in our study. This assumption is confirmed by previous studies (Hinsberger et al., 2022; Oberle et al., 2021).

2.2.7 Fu's equation

Fu et al., (2019) developed an equation to calculate Manning's n based on plant basal cover and flow depth (Eq. 5).

$$n = (a + b(1 - e^{-0.061C_v})^{1.668})h^{0.604-0.710e^{-0.219C_v}} \quad (5)$$

Where variable C_v is the ratio between the area covered by stems and the flume bed. It is considered as plant coverage in Ries et al. (2020). The plant basal cover varied between 1.25% and 30%. However, uncertainties arise in the calculation of resistance coefficients. This is because the basal elements of the vegetation may cover a smaller area than the canopy, which can result in an incomplete representation of flow resistance. The parameters a and b vary with vegetation type. In this study, the values of a and b parameters obtained by Feldmann et al., (2023) are used.

All of these equations were incorporated into the source code of OpenLISEM in order to assess the impact of various roughness methodologies on overland flow modeling.

2.3 Parameter calibration and validation

To compare the different roughness equations, we calibrate the unknown sensitive parameters of the model using one of the six rainfall experiments (Run) per site and validate the parameters using the remaining rainfall experiments. The most sensitive parameters saturated conductivity (Ksat) and average soil suction at the wetting front (Psi) are calibrated for 23 sites and 7 different roughness approaches (154 models). The parameters for the roughness functions are selected as described above and Manning's n is selected from the well-known Chow-Table (Chow, 1959). To assess the effect of these preselected values, we added Manning's n as an additional parameter, adding one model per location with 3 calibrated parameters (total 176 models). The calibration was performed with 5,000 simulations per model (880,000 models) with a distribution of the 2 or 3 parameters using the latin hypercube sampling (LHS) method using the implementation in SPOTPY (Statistical Parameter Optimization Tool) (Houska et al., 2015). The saturated hydraulic conductivity (Ksat) varies between 5 and 100 mm/hr, and the wetting front suction head (Psi) from 0 to 50 cm water column, as suggest by Gowdish and Muñoz-Carpena, (2009) for different soil types. For most locations, run 2 (100-year return period event, prewetted soil) was selected as the calibration event. Runs 1, 3, 4, 5, and 6 were selected as validation experiments. The reason for choosing Run 2 for calibration was that the soil moisture conditions during this test were neither excessively dry nor fully saturated. Since Run 2 in site 14 does not have any runoff, Run 6 is selected for calibration. Site 1 has a different order of experiments, so we are using Run 4 as the calibration run.

The best calibrated parameters are selected by ranking the model runs by their Nash-Sutcliffe efficiency. After calibrating the Ksat and Psi, models were developed for the rest experiments. The validation performance is reported as Nash-Sutcliffe efficiency (NSE) and relative bias in percent (pBias) (Table 3). High positive NSE values (close to 1) indicate that the model's predictions are in excellent agreement with the observed data. pBias with values closer to zero indicating better model performance.

Figure 2 displays a framework illustrating the calibration and simulation process of models. The simulations were iteratively repeated, considering all methods of roughness estimation. A total of 104 runs were simulated, each representing different sites or rainfall events, and repeated for various roughness methods, resulting in 832 simulations. However, models associated with Run 2 and 3 at Site 14, as well as Run 1 at Sites 12 and 16, were excluded from NSE assessment due to the absence of

https://doi.org/10.5194/egusphere-2025-5855
Preprint. Discussion started: 8 January 2026

runoff in these experimental runs. Since the observed data were zero, the NSE could not be calculated. Nevertheless, based on a comparison between the simulated hydrographs and the corresponding MSE values, the differences between the simulations and observations indicate that the model performance is acceptable.

Table 3: Criteria of NSE value (Motovilov et al., 1999) and pBias.

NSE value	pBias value	Interpretation
0.75<NSE	-10%<pBias<10%	Good
0.36<NSE<0.75	-50%<pBias<-10% or 10%<pBias<50%	Qualified
NSE<0.36	pBias<-50% or 50%<pBias	Not-Qualified

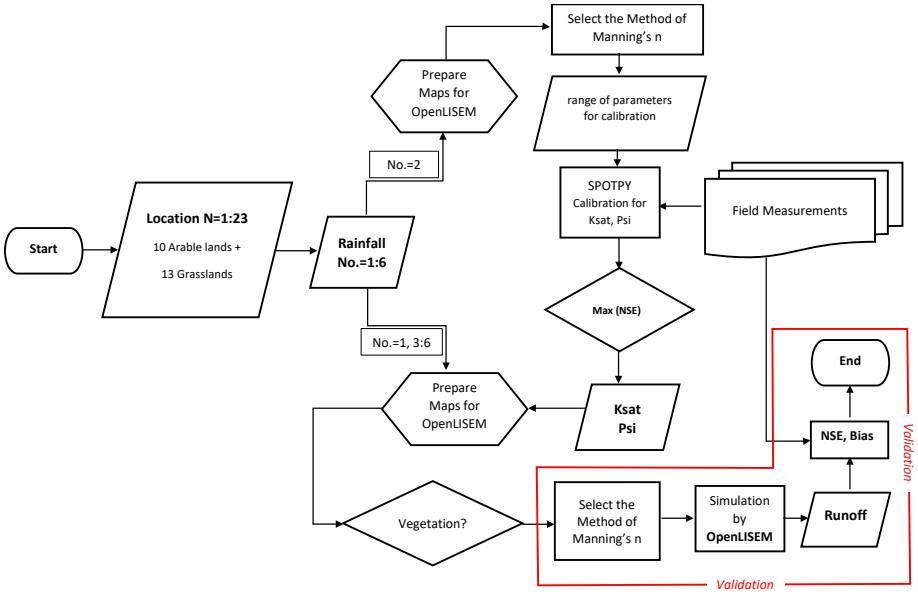

Figure 2: Framework for calibration and validation of the models.

2.4 Initial soil moisture

Initial soil moisture plays a critical role in hydrological modeling, as it directly influences the partitioning between infiltration and surface runoff. Soil moisture measured at two points at each site was used in the runoff modeling.

In addition, the sequence of six rainfall-runoff experiments (Runs 1–6, as shown in Table 2) was considered, which involved varied antecedent moisture conditions, ranging from dry to saturated. This experimental design provides a general representation of initial soil moisture states.

Therefore, in addition to point-based measurements, considering the antecedent moisture conditions of each run enhances the interpretation of simulation results and improves understanding of the hydrological model's response.

4 Result

4.1 Calibration of different roughness methods

During the calibration process using various roughness estimation methods, the simulated hydrographs generally aligned well with observed hydrographs across most sites. For instance, Figure 3 compares the calibrated hydrographs at site 6, where

https://doi.org/10.5194/egusphere-2025-5855
Preprint. Discussion started: 8 January 2026

simulated results successfully capture the temporal pattern of measured discharge for other sites; the results are presented in supplementary data. The NSE values for all sites are summarized in Figure 4. Additionally, the pBias values, computed using the calibrated Ksat and Psi parameters, are presented in Figure 5. A larger deviation of pBias from zero typically indicates a less accurate calibration.

Overall, the NSE values obtained from different roughness estimation methods showed limited variation at each site. However, Fu's method yielded poor calibration performance at Sites 5, 8, 15, 20, and 23, shown by negative NSE values and a pBias of -100. These results indicate a complete failure of the Fu method to simulate runoff at these locations, with the modeled hydrographs resulting in zero discharge.

Unfavorable calibration performance was also observed at Sites 11 and 16, where all roughness estimation methods produced relatively low NSE and pBias values. It indicates a significant discrepancy between the observed and simulated hydrographs. In contrast, the remaining sites showed satisfactory calibration results using all methods except Fu's. Excluding Sites 11 and 16, the NSE values across other locations, except Fu's method, generally ranged between 0.65 and 0.87, reflecting an acceptable level of model performance.

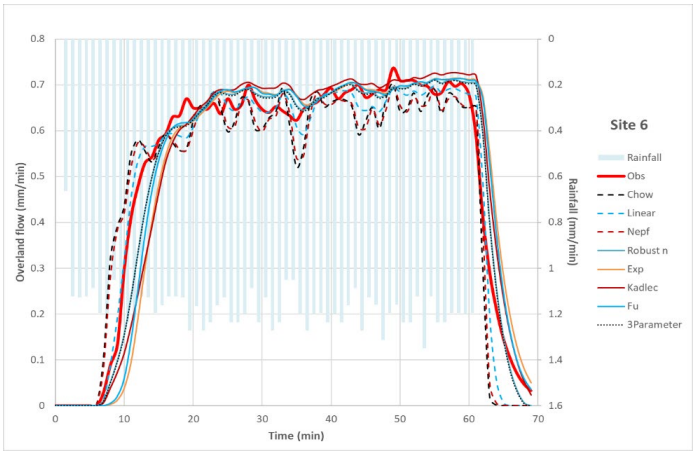

Figure 3: Comparison of the hydrograph computed using OpenLISEM with various roughness coefficient methodologies against the observed discharge.

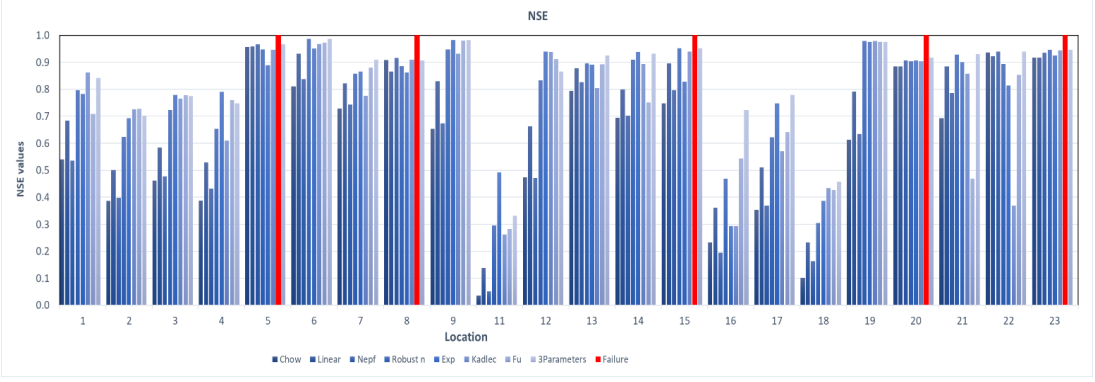

Figure 4: Maximum model performance (Nash-Sutcliffe-Efficiency) for the calibration runs of the different roughness models, separated for each site. The red bars show model failure.

https://doi.org/10.5194/egusphere-2025-5855
Preprint. Discussion started: 8 January 2026

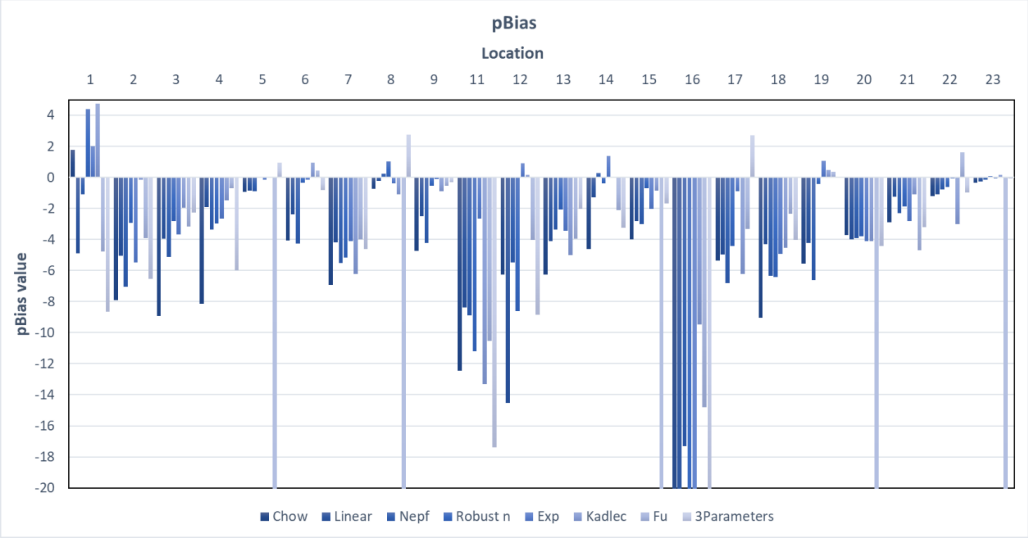

Figure 5: pBias values for parameters calibration of the different roughness models, separated for each site. Rainfall simulation Run 2 has been used for calibration, except for sites 1 and 14 (see section 3).

Runoff is generally underestimated by the model, only 13% of the runs show a slight overestimation (< 5% bias). 59% of the model runs underestimate the measured runoff by less than 5%, while 21% of the runs are underestimated by 5 – 15% of the runoff. Massive underestimation of runoff (>15%) happens outside at 5 runs using Fu's equation for surface roughness, while the runoff at site 16 is underestimated by most model runs, which is connected to the low total runoff at this site.

Table 4 presents a summary of the calibrated values of saturated hydraulic conductivity and average soil suction at the wetting front, calculated using different methods across all sites. In the case of Fu's method, the Ksat values for sites 5, 8, 15, 20, and 23 differ significantly from those obtained using other methods. These discrepancies suggest that Fu's method does not perform well in calibrating Ksat at these specific sites. The highly negative NSE values of the Fu method at these sites further support this observation. Additional results are presented in detail in the supplementary data.

A comparison of Ksat values shows that the differences between roughness methods are generally not significant, P-value=0.94, across sites. However, the values of Psi for different roughness methods show differences, P-value=0.038. By considering the soil type at each location and comparing the calibrated Ksat and Psi values with the estimates provided by Rawls et al. (1982), it becomes evident that the calibrated values are consistently higher across all sites. The only exceptions are Sites 8 and 9, which have sandy loam soils; in these cases, the calibrated values closely match those estimated by Rawls et al. (1983).

Since this discrepancy occurs across all roughness function methods, it suggests that the difference is not related to the choice of roughness method. Rather, it highlights a potential limitation of applying simplified, texture-based infiltration parameters to complex field conditions. Factors such as macropores or root development may influence soil hydraulic behavior and lead to higher infiltration rates than those predicted using generalized soil texture classifications.

Table 4: Statistical summary of calibrated parameters, Ksat (mm/hr) and Psi (cm), by site for different roughness methods.

Site No.	1	2	3	4	5	6	7	8	9	11	12
Range- Ksat	49.8- 53.9	35.5- 41.6	32.3- 37.5	30.4- 34.7	5.7- 13.2	26.0- 29.7	30.4- 33.4	7.4- 11.4	5.0- 8.6	35.8- 39.8	45.6- 47.9
Avg- Ksat	52.6	38.6	34.2	31.9	11.9	27.7	32.0	8.7	6.4	38.2	46.9
Range- Psi	1.5- 50.0	18.8- 49.9	19.5- 50.0	19.6- 49.7	0.1- 50	0.0- 48.0	16.5-49.7	0.1-19.0	11.1- 49.7	18.6- 49.9	16.0- 49.9

https://doi.org/10.5194/egusphere-2025-5855
Preprint. Discussion started: 8 January 2026

Avg- Psi	37.7	45.6	45.5	45.2	23.1	15.0	40.1	4.0	30.5	45.5	43.9
Site No.	13	14	15	16	17	18	19	20	21	22	23
Range- Ksat	38.2- 40.3	56.8- 63.7	36.4- 85.9	68.9- 70.3	24.6- 30.5	37.7- 41.2	9.0- 14.6	5.0- 94.7	5.0- 6.9	11.2- 15.5	7.2- 18.3
Avg- Ksat	39.1	60.2	43.3	69.6	28.2	39.1	11.0	16.3	5.5	14.4	8.7
Range- Psi	19.4- 49.7	18.4- 49.9	0.9- 49.7	19.9- 49.0	19.7- 49.9	19.2- 49.9	0.4- 49.9	2.4- 49.4	3.8- 47.6	0.1- 48.8	1.7- 45.4
Avg- Psi	41.8	45.5	27.0	41.5	45.8	45.2	30.8	36.8	23.3	12.7	19.4

4.2 Validation of different roughness methods

The outcomes of validation reveal that the maximum NSE range is 0.96-0.98 for different methods. Depending on the type of method, the number of models with negative NSE varies between 29 and 46, of which most of them are Run 1 and Run 5. Given that greater NSE values indicate more efficiency of the model in simulating runoff, we focused our investigation on the distribution of positive NSE values by excluding these underperforming models. Figure 6 illustrates the distribution of NSE for values greater than zero. The results indicate that the Linear and Nepf methods perform better in estimating runoff compared to the other methods; however, the differences are not statistically significant. ANOVA analysis on NSE values reveals significant differences between all group means, including Fu and Exp (P-value = 1.3e-11). In contrast, when excluding Fu and Exp from the analysis, no significant differences are observed among the remaining roughness methods (P-value = 0.4).

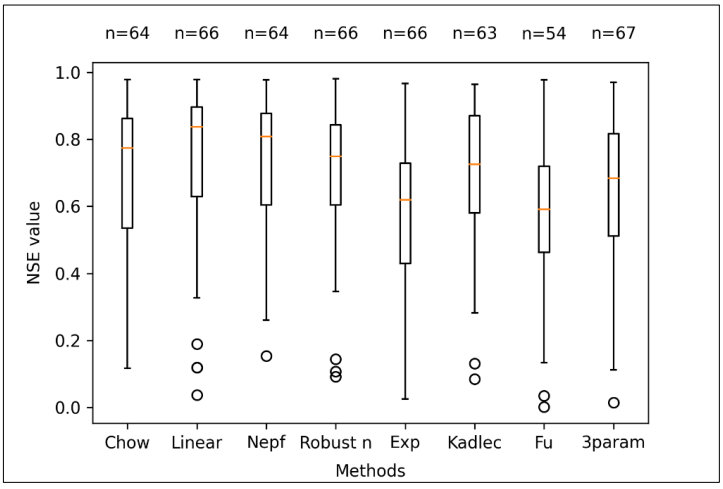

Figure 6: Distribution of the absolute values of NSE for each method of roughness for the validation runs.

The pBias results for the simulated hydrograph compared to the measured hydrograph exhibit a broad range from -100% to 100% in Figure 7. It is evident that all the methods exhibit almost a consistent trend, with the majority showcasing model bias consistently below zero. This suggests an underestimation across various roughness estimation methods. However, ANOVA analysis of the pBias values for all methods excluding Fu indicates no statistically significant difference between group means (p-value = 0.99).

https://doi.org/10.5194/egusphere-2025-5855
Preprint. Discussion started: 8 January 2026

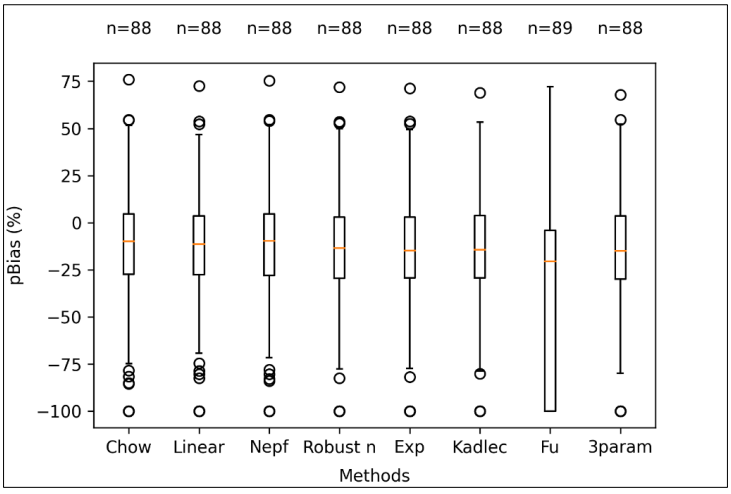

Figure 7: Distribution of the pBias for each method of roughness for the validation runs.

The analysis reveals that the Nepf, Linear, and Chow methods exhibit the most favorable performance, with 39, 38, and 34 models falling into the "Good" category based on NSE values. Conversely, for Robust n, Kadlec, 3-parameter, exponential, and Fu methods, 33, 29, 25, 15, and 9 models respectively meet the "Good" NSE criteria. Interestingly, pBias values across different methods are relatively comparable. Nepf, Chow, Linear, and 3-parameter demonstrate particularly robust performance, each with 27, 27, 26, and 26 models falling within the -10% to 10% bias range. This consistency in bias values suggests a commendable performance by these models based on pBias criteria.

4.3 Effect of initial condition and pre-event soil moisture

The validation outcomes of the roughness methods revealed Run 1 (dry conditions) and Run 5 (saturated conditions) generally shows poor model performance, with most of the methods. From the 36 model runs with negative NSE using the Nepf method, 30 are from Runs 1 and 5, as an example. Run 1 tends to overestimate runoff (positive pBias), while Run 5 underestimates it (negative pBias). The extremely low observed runoff in Run 1 makes NSE highly sensitive and often unreliable. On the other hand, these weak performance for Runs1 and Runs 5 in comparison others may because of the different on the initial condition of models with Run 2 which was selected for calibration.

4.4 Result of different vegetation coverage

The spatial proximity between the paired experimental sites offers a unique advantage in the research, providing an environment where variations in soil characteristics can be minimized, enhancing the validity of the comparative analysis.
In Figure 8, a comparative analysis between vegetation cover and Ksat, as determined by the Chow method, is presented. Comparing the pair sites reveal an increase in Ksat corresponding to more vegetation coverage. Notably, the contrast in Ksat is particularly pronounced between sites 15 and 16. Site 15, characterized as devoid of vegetation cover, displays a stark difference from site 16, boasting 100% vegetation coverage. The calibration results underscore this disparity, indicating a substantial Ksat difference of approximately 30 mm/hr. Conversely, for sites 8 and 9, this difference in Ksat is minimal. It's noteworthy that, although Ksat values may show only slight differences, another critical parameter influencing infiltration, Psi, exhibits a substantial contrast between sites 8 and 9. As presented in
Table 4, the average of Psi value in site 9 is 30.5 cm; however, this value for site 8 is 4 cm. Specifically, Psi is higher for site 9 than site 8, resulting in an enhancement in infiltration. This highlights the relationship between various parameters and their combined impact on the overall dynamics of infiltration.

https://doi.org/10.5194/egusphere-2025-5855
Preprint. Discussion started: 8 January 2026

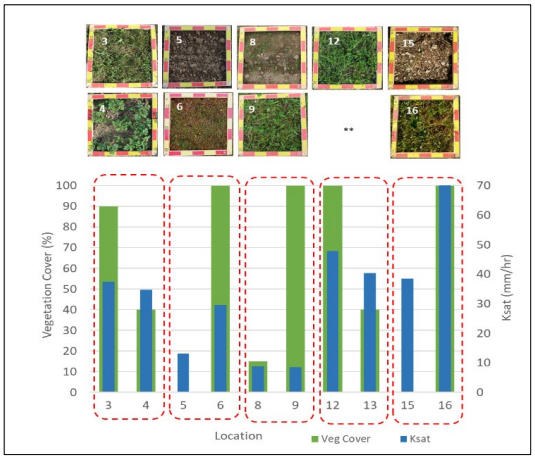

Figure 8: Saturated hydraulic conductivity values for various land uses in paired sites. ** The vegetation cover images are from Ries et al. (2020). There is no picture for Site 13.

As an example, the result for pair sites 12, 13 are shown in Figure 9. Site 12 with 100% vegetation cover and site 13 with 40% show different hydrographs both in observation and simulation. The results for Runs 2, 3, 4, and 6 are presented in this figure. For these runs, the model performs well, and the differences between observed and simulated values are not significant, the result for the other paired locations are shown in the supplementary material (Masoodi and Kraft, 2025). In these figures solid lines show the observed hydrographs and the shaded areas show the spread of results from different roughness methods. The green shaded area shows the results for the location with more vegetation cover. The spread of simulations is much larger for location 13, with less vegetation. It means in the presence of vegetation; the infiltration rate is higher than in places with less vegetation cover.

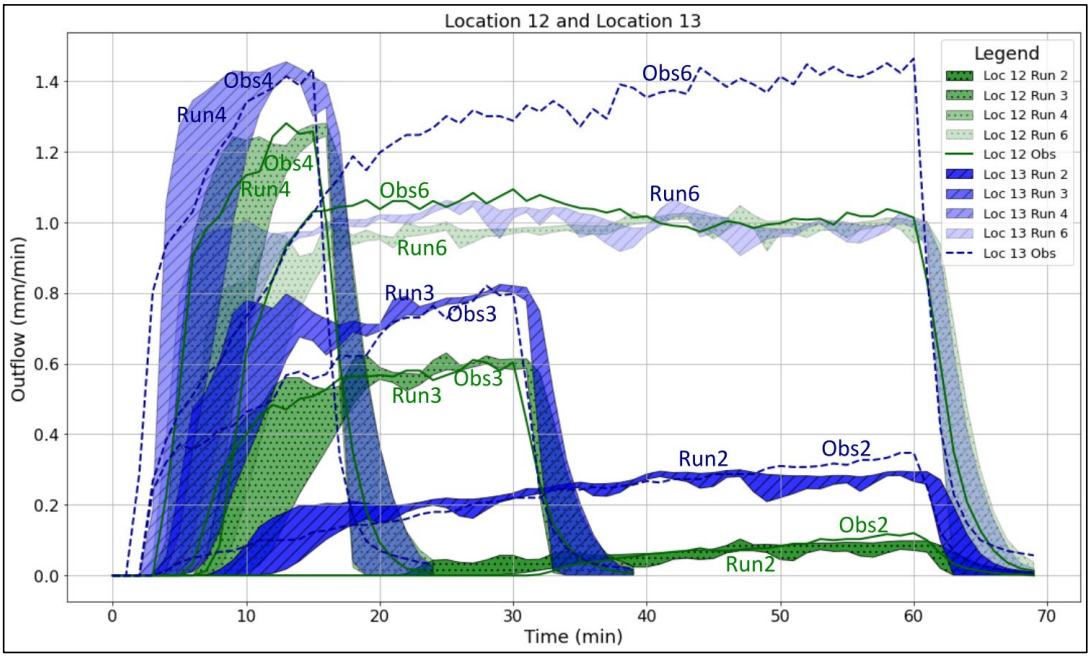

Figure 9: Comparison of observed, solid lines, and simulated hydrographs, shaded areas, at sites 12 and 13 using different roughness methods for Run2, 3, 4, and 6.

https://doi.org/10.5194/egusphere-2025-5855
Preprint. Discussion started: 8 January 2026

355 An example illustrating the model results with weak performance in Runs 1 and 5 is presented in Figure 10, which shows the outcomes for Sites 12 and 13. As discussed previously, the most models perform poorly for these two runs. A comparison between Figures 9 and 10 indicates that the weak performance in Runs 1 and 5 is not related to either the infiltration modeling or the roughness approach. This conclusion is supported by the fact that the infiltration modeling in the other runs (2, 3, 4, and 6) shows acceptable agreement between observed and simulated values. The different roughness methods cannot account for
360 the large discrepancies observed. This substantial variation may instead be attributed to the initial soil moisture conditions, which are discussed in Section 5.2.

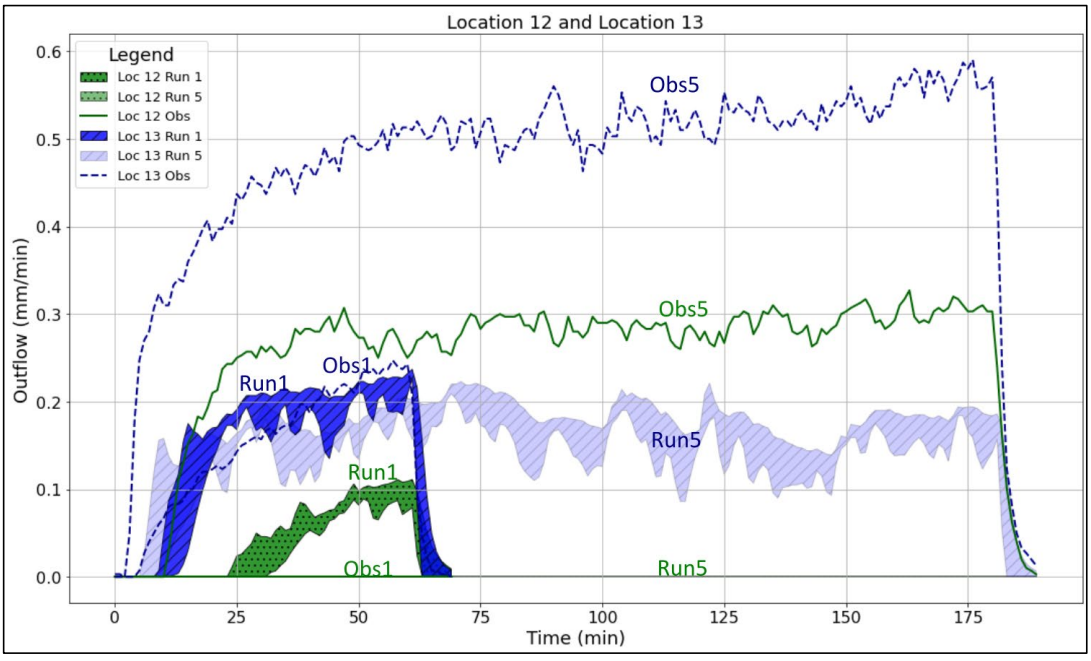

Figure 10: Comparison of observed, solid lines, and simulated hydrographs, shaded areas, at sites 12 and 13 using different
365 **roughness methods for Run1 and Run5.**

5 Discussion

5.1 Validation of different roughness methods

Our study on the validation of various roughness estimation methods revealed that models using Fu's function yielded comparatively weaker simulation results compared to experimental data. This finding is consistent with Feldmann et al. (2023),
370 who reported that Fu's equation typically produces lower NSE values, attributed primarily to the formula's limited adaptability. This limitation may stem from the fact that the function was developed based on laboratory experiments and is most applicable under similar controlled conditions where plant basal cover varied between 1.25% and 30%. Among the five sites where Fu's method completely failed during calibration, four lack vegetation cover, which may partially explain the poor model performance. An analysis of Fu's equation shows that when the value of vegetation cover, *Cv*, is less than 0.74, the
375 parameter Manning's n decreases with increasing h, whereas for *Cv* values greater than 0.74, n increases with increasing h. This shift in behaviour may explain why Fu's method performs less effectively in runs without vegetation cover. In contrast, models based on Nepf, Linear, Chow, and Robust n methods, ranked in that order, demonstrated a closer match between the simulated and observed hydrographs. Although the differences in NSE values among these latter methods are not substantial,

https://doi.org/10.5194/egusphere-2025-5855
Preprint. Discussion started: 8 January 2026

their use in roughness estimation leads to simulated hydrographs that more closely represent those derived from physical observations. One notable strength of the Nepf and Linear methods is their incorporation of water-depth-dependent relationships in estimating roughness coefficients. This is in agreement with Hinsberger et al. (2022), who emphasized the critical role of water depth in influencing hydraulic roughness and highlighted the importance of integrating this factor into catchment-scale modeling. It should be noted that in our simulations, water depth remained below vegetation height, placing the system in an emerged flow regime. Under this condition, the performance of the applied methods is considered valid; however, further investigation is required to assess their accuracy under submerged flow conditions. Additionally, the improved performance of the Nepf method may also be attributed to its inclusion of the blockage factor, which effectively represents vegetation cover and enhances the simulation of overland flow. Although originally developed for channel flow, the Nepf method demonstrates strong alignment with physically measured hydrographs in overland flow scenarios as well. Therefore, further research is warranted to assess and refine its applicability in such contexts.

Our results using the 3-parameter method indicate that increasing the number of parameters during calibration can lead to greater model complexity, which may hinder the ability to efficiently identify optimal solutions. This increase in complexity can also negatively impact overall model performance. Similar findings have been reported in previous studies involving conceptual rainfall-runoff models. For instance, Zhu et al. (2024) concluded that increasing model complexity by adding more parameters often leads to challenges in calibration, including difficulty in parameter estimation and reduced calibration efficiency. Likewise, García-Romero et al. (2019) calibrated three hydrological models with varying levels of complexity, comprising 4, 10, and 16 parameters, across nine catchments. Their results demonstrated that simpler models required fewer iterations to reach convergence, whereas more complex models demanded significantly more computational effort.

The results of methods in which roughness values are derived using the approach of Feldmann et al.'s (2023) concept, including Kadlec, Robust n, Fu, and exponential, tend to exhibit greater deviation from experimental data. Figure 11 illustrates a comparison of the simulated hydrographs using different roughness estimation methods for all experiments conducted at site 9. Site 9 is specifically chosen because its hydrographs were featured in Feldmann et al.'s (2023) study, and the calibration for the four methods employed therein is superior to that of the Linear and Nepf methods, as depicted in Figure 4. Figure 11 demonstrates that Kadlec, Robust n, Exponential, and Fu methods approximate the falling limb of the hydrograph more closely to the observed hydrograph compared to the Linear, Nepf, and Chow methods. It's essential to note that the base of optimization in Feldmann et al. (2023) study is on the falling limb of the hydrograph, where it shows superior performance. However, the NSE results for the entire hydrograph are better for Nepf, Linear, and Chow.

https://doi.org/10.5194/egusphere-2025-5855
Preprint. Discussion started: 8 January 2026

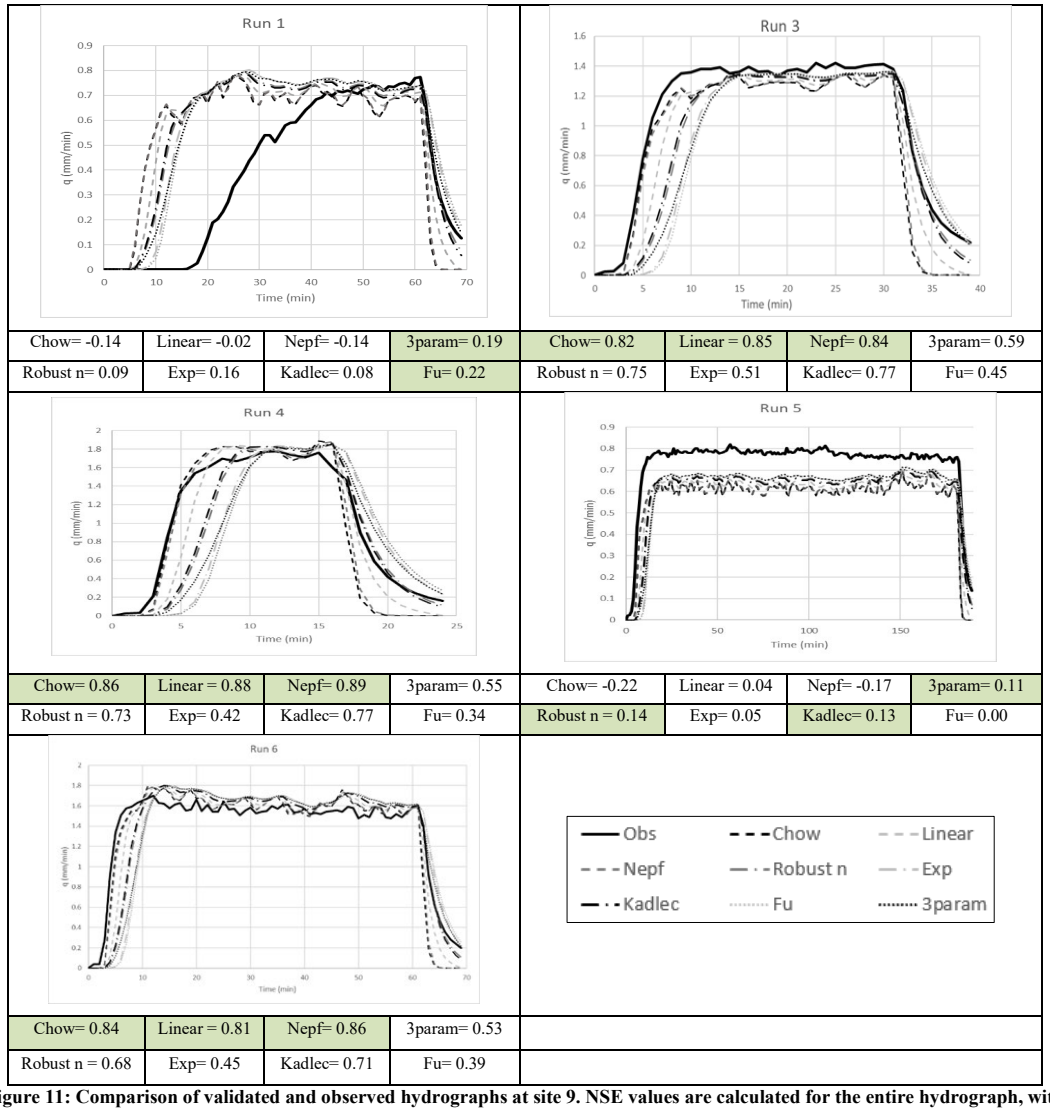

Chow= -0.14	Linear= -0.02	Nepf= -0.14	3param= 0.19	Chow= 0.82	Linear = 0.85	Nepf= 0.84	3param= 0.59
Robust n= 0.09	Exp= 0.16	Kadlec= 0.08	Fu= 0.22	Robust n = 0.75	Exp= 0.51	Kadlec= 0.77	Fu= 0.45
Chow= 0.86	Linear = 0.88	Nepf= 0.89	3param= 0.55	Chow= -0.22	Linear = 0.04	Nepf= -0.17	3param= 0.11
Robust n = 0.73	Exp= 0.42	Kadlec= 0.77	Fu= 0.34	Robust n = 0.14	Exp= 0.05	Kadlec= 0.13	Fu= 0.00
Chow= 0.84	Linear = 0.81	Nepf= 0.86	3param= 0.53				
Robust n = 0.68	Exp= 0.45	Kadlec= 0.71	Fu= 0.39				

Figure 11: Comparison of validated and observed hydrographs at site 9. NSE values are calculated for the entire hydrograph, with green cells indicating methods that have higher NSE values.

This discrepancy may stem from the approach's omission of vegetation effects on infiltration parameters. Feldmann et al. (2023) proposed a more constrained roughness estimation method by identifying overlapping solution spaces and reducing the overall solution space to enhance reliability. Their methodology focuses on the falling limb of the hydrograph, where infiltration is assumed to remain relatively constant. They fitted an infiltration function to this segment of the hydrograph and derived infiltration rates without explicitly considering vegetation's role in modifying these rates. However, our findings suggest that vegetation significantly influences not only roughness coefficients but also key infiltration parameters, such as Ksat, thereby affecting overall infiltration dynamics. These results are consistent with the conclusions of Gao et al. (2023), who emphasized that soil hydraulic properties are influenced by both water movement and ecosystem activity. They highlighted the root zone as a critical component with substantial storage capacity, playing a key role in regulating how precipitation is partitioned into streamflow. According to their framework, vegetation actively alters soil characteristics to

https://doi.org/10.5194/egusphere-2025-5855
Preprint. Discussion started: 8 January 2026

optimize water availability, which underscores the importance of incorporating ecosystem and soil interactions into hydrological modeling.

5.2 Effect of initial condition and pre-event soil moisture

Our results highlight the significant influence of antecedent soil moisture conditions on runoff modeling accuracy, particularly in Runs 1 and 5 (Figure 10). Run 1 began with unusually dry soil, while Run 5 followed a sequence of moderate rainfall events (Runs 2, 3, and 4), leading to substantially wetter initial conditions. Both exhibited significant deviations between simulated and observed runoff, suggesting that the model struggled to replicate hydrological responses under extreme antecedent moisture states.

These findings are in agreement with Brocca et al. (2008), who demonstrated that pre-event soil moisture is a key determinant of runoff depth and peak discharge. Their conceptual soil water balance model incorporates Green–Ampt infiltration and non-linear drainage mechanism. In our study, models calibrated under a specific initial moisture condition (e.g., Run 2) yielded more reliable results when validated against runs with comparable antecedent states (e.g., Runs 3, 4, and 6). However, performance declined when these models were applied to scenarios with contrasting initial soil moisture (e.g., Runs 1 and 5), emphasizing the model's sensitivity to calibration context. Feldmann et al. (2023) observed a decrease in median deviation from the roughness mean in Run 5 during prolonged rainfall events and attributed this to the formation of flow paths influencing roughness values. However, we suggest that this reduction may be linked to the effects of antecedent rainfall on runoff response, and not to rainfall intensity or flow path development. This is supported by the behavior in Run 6, where the deviation from the roughness mean increased again despite continued rainfall, indicating that the changes are not solely due to flow path formation.

Zehe and Blöschl (2004) investigated how uncertainty in initial soil moisture affects hydrologic responses at the plot and catchment scales, using a physical model that accounts for transitions between matrix and preferential flow. Their simulation results showed that model predictability is lowest near the soil moisture threshold separating these flow regimes in the soil. In the present study, Runs 1 and 5 represent transitional soil moisture conditions similar to those reported by Zehe and Blöschl (2004). Comparing the results of these runs highlight the difficulty of accurately predicting hydrological responses under uncertain initial soil moisture conditions. These findings are consistent with Zehe and Blöschl (2004).

We found that the response of our model under different soil moisture condition has uncertainty, particularly when soil approaches saturation. This discrepancy may stem from limitations in infiltration modeling under these conditions. For example, the Green–Ampt approach assumes an initially dry soil profile, which can result in unrealistic infiltration estimates during high-intensity storms on already wet soils. This limitation highlights the need for improved infiltration models that better accommodate a range of antecedent soil moisture conditions.

5.3 Result of different vegetation coverage

The findings presented in our study validate previous research, which has emphasized the differences in near-surface Ksat across various land covers (Zwartendijk et al., 2023). These differences result in different shaping perched water table dynamics and overland flow responses (Ghimire et al., 2020; van Meerveld et al., 2021; Zwartendijk et al., 2020, 2023). The study conducted by Wu et al. (2024) on the temporal variability of Ksat throughout the growing season revealed the significant influence of root growth. They explained that root development improves soil pore connectivity, thereby increasing Ksat. Consequently, top-soil infiltration rates typically experience improvement, resulting in reduced overland flow and a decrease or delayed runoff response to rainfall events (van Meerveld et al., 2019). Jarvis et al. (2013) identified land use as one of the top three most significant predictors for Ksat. They concluded that intensive cultivation of arable land significantly diminishes topsoil hydraulic conductivity compared to perennial agriculture, natural vegetation, and forests, by approximately 2–3 times. They attributed this reduction to the disruptive effects of tillage on macropores, including faunal and root bio pores.

https://doi.org/10.5194/egusphere-2025-5855
Preprint. Discussion started: 8 January 2026

Our research indicates that in the presence of vegetation, not only is surface roughness important in hydrological processes, but the increase in Ksat also significantly influences the response of hydrological models to runoff. This highlights the critical importance of incorporating vegetation-induced changes in hydraulic conductivity when modeling runoff responses. A great difference from the related studies by Feldmann et al. (2023) and Hinsberger et al. (2022) is the use of a model with an integrated infiltration model. Classical engineering models for surface runoff and most commercial models deal with infiltration as a process that can be determined a priori and subtracted directly from the rainfall. The ability of the soil to absorb water is dynamic in nature but is often oversimplified which led to inaccuracies (Beven, 2021). We used the dynamic Green-Ampt Infiltration model from OpenLISEM, and which captured the infiltration process in the majority of cases.

Thus, the result is both a validation of expected trends and a contribution to understanding the importance of incorporating Ksat variability in hydrological models. While we observe the strong effect of vegetation on infiltration capacity, our data set is not sufficient to come up with a robust estimate to quantify this effect.

6 Conclusion

Our study evaluates of various roughness estimation methods and their impact on hydrological modeling using OpenLISEM. Through model calibration and validation, we have gained valuable insights into the performance of each roughness method. Our findings reveal that certain methods, such as Linear, constant Manning's n proposed by Chow, and the physical base method proposed by Luhar and Nepf (2013), demonstrate favorable performance in reproducing observed hydrological data, as evidenced by high NSE values and minimal bias. Methods like Fu's equation exhibit weaker simulation results, attributed to its limited adaptability and lower NSE values. The methods have been developed for submerged vegetation, but in our study, as for sheet flow events on vegetated surfaces in general, the runoff depth observed in this study did not exceed the height of the vegetation.

We observed notable differences in near-surface saturated hydraulic conductivity across various vegetation covers. The differences observed in model outcomes between various runs in one site highlight the need for improved models that accurately account for infiltration for varying antecedent conditions. Surface runoff models use vegetation solely as a parameter of surface roughness and rainfall runoff models as a transpiration parameter. For the effect of storm events in developed landscapes, vegetation is an important regulator of infiltration, yet this effect is not well represented in current models. Future studies should investigate which rainfall events yield better results when included in the calibration process. Selecting the most representative rainfall event should consider both dry and saturated soil moisture conditions, enhancing the accuracy of hydrological modeling. It is important to acknowledge the inherent limitations of hydrological models, which may influence our results. For instance, this model does not explicitly consider the effects of increased water pressure at higher water levels, which could also impact infiltration dynamics.

Supplementary and Code availability.

Data are published in the zenodo.org repository under https://doi.org/10.5281/zenodo.17572291

Code is available on https://github.com/philippkraft/openlisem/tree/modified_manning_console

Author contributions. AM: Programming, Simulation, Data analysis, Manuscript draft writing.
PK: Conceptualization, Funding acquisition, Software development, Manuscript review and editing.

Competing interests. The authors declare that they have no conflict of interest.

Acknowledgements. This research was funded by Hessisches Landesamt für Naturschutz, Umwelt und Geologie (HLNUG) for the project "Innovativer Erosionsschutz für Hessen unter Klimawandel" (Z1-15C c 01.02.).

https://doi.org/10.5194/egusphere-2025-5855
Preprint. Discussion started: 8 January 2026

References

Ajayi, A. E., Faloye, O. T., Reinsch, T., and Horn, R.: Changes in soil structure and pore functions under long term/continuous grassland management, Agric. Ecosyst. Environ., 314, 107407, https://doi.org/10.1016/j.agee.2021.107407, 2021.

Baartman, J. E. M., Jetten, V. G., Ritsema, C. J., and de Vente, J.: Exploring effects of rainfall intensity and duration on soil erosion at the catchment scale using openLISEM: Prado catchment, SE Spain, Hydrol. Process., 26, 1034–1049, https://doi.org/10.1002/hyp.8196, 2012.

Beven, K.: The era of infiltration, Hydrol. Earth Syst. Sci., 25, 851–866, https://doi.org/10.5194/hess-25-851-2021, 2021.

Brocca, L., Melone, F., and Moramarco, T.: On the estimation of antecedent wetness conditions in rainfall–runoff modelling, Hydrol. Process., 22, 629–642, https://doi.org/10.1002/hyp.6629, 2008.

Chow, V. T.: Open-Channel Hydraulics, McGraw-Hill Book Co., NY, USA, 110 pp., 1959.

Dalledonne, G. L., Kopmann, R., and Brudy-Zippelius, T.: Uncertainty quantification of floodplain friction in hydrodynamic models, Hydrol. Earth Syst. Sci., 23, 3373–3385, https://doi.org/10.5194/hess-23-3373-2019, 2019.

D'Ippolito, A., Calomino, F., Alfonsi, G., and Lauria, A.: Flow Resistance in Open Channel Due to Vegetation at Reach Scale: A Review, Water, 13, 116, https://doi.org/10.3390/w13020116, 2021.

Drewniak, B. A.: Simulating Dynamic Roots in the Energy Exascale Earth System Land Model, J. Adv. Model. Earth Syst., 11, 338–359, https://doi.org/10.1029/2018MS001334, 2019.

Feldmann, D., Laux, P., Heckl, A., Schindler, M., and Kunstmann, H.: Near surface roughness estimation: A parameterization derived from artificial rainfall experiments and two-dimensional hydrodynamic modelling for multiple vegetation coverages, J. Hydrol., 617, 128786, https://doi.org/10.1016/j.jhydrol.2022.128786, 2023.

Fu, S., Mu, H., Liu, B., Yu, X., and Liu, Y.: Effect of plant basal cover on velocity of shallow overland flow, J. Hydrol., 577, 123947, https://doi.org/10.1016/j.jhydrol.2019.123947, 2019.

Gao, H., Fenicia, F., and Savenije, H. H. G.: HESS Opinions: Are soils overrated in hydrology?, Hydrol. Earth Syst. Sci., 27, 2607–2620, https://doi.org/10.5194/hess-27-2607-2023, 2023.

García-Romero, L., Paredes-Arquiola, J., Solera, A., Belda, E., Andreu, J., and Sánchez-Quispe, S. T.: Optimization of the Multi-Start Strategy of a Direct-Search Algorithm for the Calibration of Rainfall–Runoff Models for Water-Resource Assessment, Water, 11, 1876, https://doi.org/10.3390/w11091876, 2019.

Ghimire, C. P., Zwartendijk, B. W., Ravelona, M., Lahitiana, J., and Van Meerveld, H. J.: Hydrological and meteorological data for three plots with different vegetation near Andasibe, Madagascar, 2014-2015, https://doi.org/10.5285/5D080FEF-613A-4F24-A613-B249CCDD12BF, 2020.

Green, J. C.: Modelling flow resistance in vegetated streams: review and development of new theory, Hydrol. Process., 19, 1245–1259, https://doi.org/10.1002/hyp.5564, 2005.

Hessel, R., Jetten, V., Liu, B., Zhang, Y., and Stolte, J.: Calibration of the LISEM model for a small Loess Plateau catchment, CATENA, 54, 235–254, https://doi.org/10.1016/S0341-8162(03)00067-5, 2003.

Hinsberger, R., Biehler, A., and Yörük, A.: Influence of Water Depth and Slope on Roughness—Experiments and Roughness Approach for Rain-on-Grid Modeling, Water, 14, 4017, https://doi.org/10.3390/w14244017, 2022.

Houska, T., Kraft, P., Chamorro-Chavez, A., and Breuer, L.: SPOTting Model Parameters Using a Ready-Made Python Package, PLOS ONE, 10, e0145180, https://doi.org/10.1371/journal.pone.0145180, 2015.

Jain, M. K., Kothyari, U. C., and Ranga Raju, K. G.: A GIS based distributed rainfall–runoff model, J. Hydrol., 299, 107–135, https://doi.org/10.1016/j.jhydrol.2004.04.024, 2004.

Jarvis, N., Koestel, J., Messing, I., Moeys, J., and Lindahl, A.: Influence of soil, land use and climatic factors on the hydraulic conductivity of soil, Hydrol. Earth Syst. Sci., 17, 5185–5195, https://doi.org/10.5194/hess-17-5185-2013, 2013.

Jetten, V.: LISEM, Limburg Soil Erosion Model, User's Manual, University of Utrecht, 2002.

https://doi.org/10.5194/egusphere-2025-5855
Preprint. Discussion started: 8 January 2026

Lu, H., Yuan, W., and Chen, X.: A Processes-Based Dynamic Root Growth Model Integrated Into the Ecosystem Model, J. Adv. Model. Earth Syst., 11, 4614–4628, https://doi.org/10.1029/2019MS001846, 2019.

Luhar, M. and Nepf, H. M.: From the blade scale to the reach scale: A characterization of aquatic vegetative drag, Adv. Water Resour., 51, 305–316, https://doi.org/10.1016/j.advwatres.2012.02.002, 2013.

Masoodi, A. and Kraft, P.: Simulation Results of Hydrographs for Different Surface Roughness Approaches Using OpenLISEM, https://doi.org/10.5281/ZENODO.17572291, 2025.

van Meerveld, H. J. (Ilja), Zhang, J., Tripoli, R., and Bruijnzeel, L. A.: Effects of Reforestation of a Degraded *Imperata* Grassland on Dominant Flow Pathways and Streamflow Responses in Leyte, the Philippines, Water Resour. Res., 55, 4128–4148, https://doi.org/10.1029/2018WR023896, 2019.

van Meerveld, H. J. (Ilja), Jones, J. P. G., Ghimire, C. P., Zwartendijk, B. W., Lahitiana, J., Ravelona, M., and Mulligan, M.: Forest regeneration can positively contribute to local hydrological ecosystem services: Implications for forest landscape restoration, J. Appl. Ecol., 58, 755–765, https://doi.org/10.1111/1365-2664.13836, 2021.

Motovilov, Y. G., Gottschalk, L., Engeland, K., and Rodhe, A.: Validation of a distributed hydrological model against spatial observations, Agric. For. Meteorol., 98–99, 257–277, https://doi.org/10.1016/S0168-1923(99)00102-1, 1999.

Mu, H., Yu, X., Fu, S., Yu, B., Liu, Y., and Zhang, G.: Effect of stem cover on hydraulic parameters of overland flow, J. Hydrol., 577, 123964, https://doi.org/10.1016/j.jhydrol.2019.123964, 2019.

Oberle, P., Kron, A., Kerlin, T., Rodriguez, E. R., and Nestmann, F.: Diskussionsbeitrag zur Fließwiderstandsparametrisierung zur Simulation von Oberflächenabflüssen infolge Starkregen, in: Dresdner Wasserbauliche Mitteilungen 65, Technische Universität Dresden, Institut für Wasserbau und technische Hydromechanik (Hg.): Wasserbau zwischen Hochwasser und Wassermangel, 129–139, 2021.

Oberle, P., Jakobs, T., and Franca, M. J.: Experimentelle Untersuchungen von Dünnschichtabfluss auf natürlichem Grasland, in: 47. Dresdner Wasserbaukolloquium, Von der Technischen Hydromechanik zu Environmental Fluid Dynamics, Dresden, Technische Universität Dresden, Institut für Wasserbau und technische Hydromechanik (Dresdner Wasserbauliche Mitteilungen, 72), 45–53, 2024.

Peel, M. C.: Hydrology: catchment vegetation and runoff, Prog. Phys. Geogr. Earth Environ., 33, 837–844, https://doi.org/10.1177/0309133309350122, 2009.

Rawls, W. J., Brakensiek, D. L., and Miller, N.: Green-ampt Infiltration Parameters from Soils Data, J. Hydraul. Eng., 109, 62–70, https://doi.org/10.1061/(ASCE)0733-9429(1983)109:1(62), 1983.

Ries, F., Kirn, L., and Weiler, M.: Runoff reaction from extreme rainfall events on natural hillslopes: a data set from 132 large-scale sprinkling experiments in south-western Germany, Earth Syst. Sci. Data, 12, 245–255, https://doi.org/10.5194/essd-12-245-2020, 2020.

Ruiz Rodriguez, E.: Umgang mit Starkniederschlägen in Hessen. Auszug aus dem 3. Zwischenbericht, Hochschule RheinMain, Wiesbaden, 2017.

Starkloff, T. and Stolte, J.: Applied comparison of the erosion risk models EROSION 3D and LISEM for a small catchment in Norway, CATENA, 118, 154–167, https://doi.org/10.1016/j.catena.2014.02.004, 2014.

Vargas-Luna, A., Crosato, A., and Uijttewaal, W. S. J.: Effects of vegetation on flow and sediment transport: comparative analyses and validation of predicting models: EFFECTS OF VEGETATION ON FLOW AND SEDIMENT TRANSPORT, Earth Surf. Process. Landf., 40, 157–176, https://doi.org/10.1002/esp.3633, 2015.

Wu, X., Yang, Y., He, T., Wang, Y., Liu, B., and Liu, Y.: Temporal variability of saturated hydraulic conductivity on a typical black soil slope of northeast China, CATENA, 236, 107742, https://doi.org/10.1016/j.catena.2023.107742, 2024.

Zehe, E. and Blöschl, G.: Predictability of hydrologic response at the plot and catchment scales: Role of initial conditions, Water Resour. Res., 40, 2003WR002869, https://doi.org/10.1029/2003WR002869, 2004.

Zhang, S., Zhang, J., Liu, Y., and Liu, Y.: Effects of farmland vegetation row direction on overland flow hydraulic characteristics, Hydrol. Res., 49, 1991–2001, https://doi.org/10.2166/nh.2018.020, 2018.

https://doi.org/10.5194/egusphere-2025-5855
Preprint. Discussion started: 8 January 2026

Zhu, S., Maier, H. R., Zecchin, A. C., Thyer, M. A., and Guillaume, J. H. A.: Improved understanding of calibration efficiency, difficulty and parameter uniqueness of conceptual rainfall runoff models using fitness landscape metrics, J. Hydrol., 639, 131586, https://doi.org/10.1016/j.jhydrol.2024.131586, 2024.

Zwartendijk, B. W., van Meerveld, H. J., Ghimire, C. P., Ravelona, M., Lahitiana, J., and Bruijnzeel, L. A.: Soil water- and overland flow dynamics in a tropical catchment subject to long-term slash-and-burn agriculture, J. Hydrol., 582, 124287, https://doi.org/10.1016/j.jhydrol.2019.124287, 2020.

Zwartendijk, B. W., van Meerveld, H. J., Teuling, A. J., Ghimire, C. P., and Bruijnzeel, L. A.: Rainfall-runoff responses and hillslope moisture thresholds for an upland tropical catchment in Eastern Madagascar subject to long-term slash-and-burn practices, Hydrol. Process., 37, e14937, https://doi.org/10.1002/hyp.14937, 2023.